

Numerical Estimations of Wave Reflection Coefficients for Irregular Waves Over Submerged Obstacles

Ruey-syan Shih¹, Chung-ren Chou², John. Z. Yim²

1. Tung Nan Institute of Technology, Taipei, TAIWAN, China
2. National Taiwan Ocean University, Keelung, TAIWAN, China

ABSTRACT

Numerical simulations of irregular waves propagate over a set of submerged obstacles with various conditions are investigated in this study by means of boundary element method. The algorithm was based on the Lagrangian description with finite difference adopted for the approximation of time derivative. The accuracy of the model was first verified by studying the case of irregular waves propagating the water tank without any obstacle. Moreover, sets of submerged breakwaters are fixed under the water tank for investigation. An artificial absorbing beach represents here as sponge zone is employed at the other end of the flume to minimize the reflection effects. Power spectrum of Brestschneider-Mitsuyasu type defined by significant wave height, $H_{1/3}$, and significant wave period, $T_{1/3}$, employed for the condition of incident waves was chosen for the generation of irregular waves. Time histories of water elevations are measured with numerous pseudo wave gages on the free water surface, by comparing the spectra of these gages with the target, also refer to the methods for estimation of irregular incident and reflected waves in random sea presented by Goda & Suzuki, the dissipative efficiency of the breakwaters are therefore investigated. Gauges with different position are tested for their suitability of the estimations of reflection coefficients for irregular wave. In this paper, the results demonstrated the effectiveness of the estimation of reflection coefficient for random waves, which clarify the numerical model a feasible scheme.

KEY WORDS: Boundary element method, Numerical Wave Tank, Reflection coefficient, Irregular wave, Submerged obstacle.

INTRODUCTION

In virtue of the high-speed development of science and technology of electronic calculator nowadays, numerous numerical models are being enthusiastically established for the estimations of oceanic physical characteristics, which provided several reliable statistics for the design and construction of coastal structures. The sea wall, jetty and detached breakwaters are traditionally adopted as absorbing facilities for the elimination of water wave energies. In Taiwan, starting from

somewhere around the 80's, the construction of coastal jetty and detached breakwaters were progressively adopted for coastal protection. Formerly, considerable quantities of armor units were piled outside the protecting embankment to achieve efficiency of absorptions, which in fact accomplished the purpose and ensure inland safety, effectiveness yet destroyed the landscape and ecological environment. In view of the preserving of natural landscape and the enforcement of so-called "amenity-oriented policy" recently, many constructions are being substituted by ecological engineering method. Modifications can now be found by the seashore such as submerged breakwaters, artificial submerged reefs, artificial beach, amenity-oriented sea dyke, etc., the exploitation of submerged breakers may not only increase the damage to the landscape, but also enforced waves to break either above or behind the obstacles. The investigation of irregular waves propagate over a set of submerged obstacles with various positions are investigated in this study by means of boundary element method. The elimination of wave energy by submerged obstacles have being extensively investigated by many researchers, e.g., an experimental investigation on the submerged dike are presented formerly by Nakamura et al. (1966), which mainly deals with the damping effect due to breaking on the submerged dike. The probability density function of the wave heights and periods as well as the shape of the spectrum was discussed by Lee and Black (1978) using spectral analysis and zero-up-crossing procedure.

Regarding the estimations of reflection coefficients, a well known method presented by Goda and Suzuki (1976) to resolve the incident and reflected waves from the records of composite waves in a random wave field has been extensively adopted as a way to estimate the reflection coefficient in the laboratory, where the water elevation was measured by a two probe system. The incident and reflected spectra was also calculated by a least square method presented by Mansard and Funke (1980) using the data of a simultaneous measurement of water elevation by three probes. Similarly, Gaillard et al. (1980) published a method of evaluation of both the incident and reflected wave spectra in laboratory experiments and/or field investigation by using the analysis of the wave records obtained by three probes array, and their results are also found to be reliable. Based on the use of digital filters, Frigaard and Brorsen (1995) presented a new method for separating irregular into incident and reflected waves, efficiency of the model is demonstrated

by both the physical and numerical test. The above method was modified later by Baldock and Simmonds (1999) to account for normally incident linear waves propagating over a sloping bathymetry, which the amplitude and phase change between two probes was determined using linear shoaling theory. The estimation of the reflection coefficients in a wave flume with the water evaluations measured by three probes was studied by Sanchez (2000) using a complex function. Shu et al (2001) developed a model that predicts the reflections for irregular waves normally incident upon a perforated-wall caisson breakwater by using an eigenfunction expansion method. Considering the influence due to bounded beach, Doclos and Clément (2003) present a method for the estimation of transmission and reflection coefficients for water wave in a small basin by extending the Goda two probes method to three probes.

The generation and propagation of irregular waves in a 2D wave basin are being investigated by Chou et al. since 1998, a Mitsuyasu-Bretschneider type spectrum is chosen as target. However, due probably to the reflected wave from the vertical wall, only less than fifty sampling waves could be generated. This problem are further improved by employing a sponge zone at the end of the flume (Chou et al, 2001), the generation of irregular wave revealed that the improved present numerical scheme are capable of describing the propagation of irregular waves quite satisfactorily (Shih et al, 2004). In this paper, the deformations of irregular waves over submerged obstacles with its application to reflection coefficient estimations are investigated.

NUMERICAL METHOD & THEORETICAL BACKGROUND

2.1 Governing Equation and Basic Assumptions

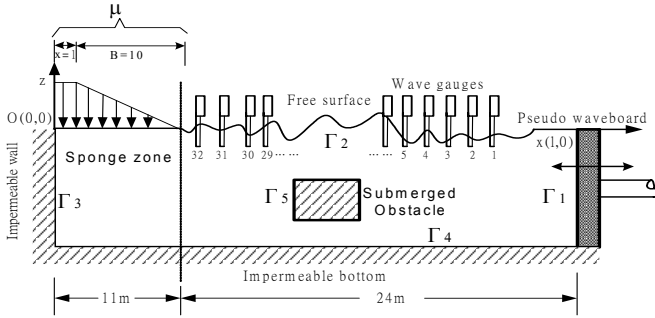


Fig.1 Definition sketch of Numerical Wave Flume

As shown schematically in Fig.1, Numerical wave flume is confined in a region composed of a piston type wave generator located at the right, the undisturbed free water surface, an impermeable vertical wall and bottom and a impermeable obstacle. The origin is located on the still water surface with the z-axis pointed positively upwards and x-axis pointed positively right. Vertical wall is adopted at the left end of the flume so as to bear more resemblance to the physical wave generation. The regime of interest is bounded by the pseudo wave board Γ_1 , the free water surface Γ_2 , the vertical wall Γ_3 , the impermeable bottom floor Γ_4 and impermeable submerged obstacle Γ_5 . Boundaries are discretized as linear elements. Fluids within the region are conventionally assumed as incompressible, inviscid, and irrotational. According to Green's second identity, the velocity potential $\Phi(x,z,t)$ must satisfies the following Laplace equation:

$$\frac{\partial^2 \Phi}{\partial x^2} + \frac{\partial^2 \Phi}{\partial z^2} = 0 \quad (1)$$

The boundary conditions on the undisturbed free water surface can be obtained from the nonlinear kinematic and dynamic conditions and are expressed as:

$$u = \frac{Dx}{Dt} = \frac{\partial \Phi}{\partial x} \quad (2)$$

$$w = \frac{Dz}{Dt} = \frac{\partial \Phi}{\partial z} \quad (3)$$

$$\frac{D\Phi}{Dt} + g\zeta - \frac{1}{2} \left[\left(\frac{\partial \Phi}{\partial x} \right)^2 + \left(\frac{\partial \Phi}{\partial z} \right)^2 \right] + \frac{P}{\rho} = 0 \quad (4)$$

where $D(\cdot)$ is the Lagrangian derivative, g is the gravitational acceleration, with ζ representing the surface fluctuation, ρ is the density of water, and P is the gage pressure on the water surface, on the non-absorbing area, the atmospheric pressure term is generally assumed to be constant, e.g., $P = 0$.

On the left side of the flume, referred to as the sponge zone, the absorption of free surface waves including varies conditions are discussed by Cao et al. (1993). In the present research, the value of P was defined proportional to the potential on the free water, thus, $P(x, \zeta)$ is expressed as:

$$P(x, \zeta) = \mu(x)\Phi(\xi, \eta, t) \quad (5)$$

$\mu(x)$ is the beach absorption function, which is assumed to vary smoothly along section $x_x - x_B$, but remains constant after x_x , the absorbing coefficient can thus be expressed as:

$$\mu(x, t) = \mu_0(t) \rho \left(\frac{x_B - x}{B} \right)^\alpha, \quad x_x < x < x_B \quad (6)$$

$$\mu(x, t) = \mu_0(t) \rho, \quad x \leq x_x \quad (7)$$

where $B = x_x - x_B$ is the length of varying-value section. As can be seen from Figure 1, a linear absorption parameter is adopted in this paper, i.e. $\alpha = 1$.

The boundary condition on the wave-paddle is obtained by matching the horizontal velocities $U(t)$ of the paddle and that of the fluid through the following association:

$$\bar{\Phi} = \frac{\partial \Phi}{\partial n} = -U(t) \quad \text{on } \Gamma_1 \quad (8)$$

where n is the unit outward normal vector, the value of $U(t)$ will be discussed in the following section.

Since both the particle velocity is null in the normal direction on the impermeable vertical wall, the bottom floor and the submerged obstacle, the condition is therefore prescribed as:

$$\frac{\partial \Phi}{\partial n} = 0 \quad \text{on } \Gamma_3, \Gamma_4 \text{ and } \Gamma_5 \quad (9)$$

2.2 Random Wave Simulations

The Bretschneider-Mitsuyasu spectrum is used as the target spectrum for the generation of irregular waves, which can be expressed as:

$$S_0(f) = 0.257 H_{1/3}^2 T_{1/3}^{-4} f^{-5} \exp[-1.03(T_{1/3} f)^{-4}] \quad (10)$$

where $H_{1/3}$ is the significant wave height, $T_{1/3}$ is the significant wave period, and f is the frequency. According to Goda (2000), the spectral peak frequency, f_p , is related to the significant wave period, T_p :

$$f_p = 1/T_p \quad (11)$$

where $T_p \cong 1.05T_{1/3}$. Similar to that in physical applications of the wave generation theory, a transfer function must be multiplied to obtain the spectrum for the motion of the numerical wave generator, thus:

$$S(f) = \alpha(f)^2 \cdot S_0(f) \quad (12)$$

$\alpha(f)$ denotes the transfer function of wave amplitude and the stroke of wave paddle, whereas in the present study, a piston type wave generator was investigated, hence,

$$\alpha(f) = \frac{\sinh kh \cosh kh + kh}{2 \sin^2 kh} \quad (13)$$

k is the wave number, h is the water depth. Neglect the period which are excessively small or large, i.e. the associate period resolution can be express as:

$$T_{\min} < T < T_{\max} \quad (14)$$

where $T_{\min} = 0.5\text{sec}$ and $T_{\max} = 4.5\text{sec}$ was chosen presently to avoid unexpected long waves as well as short waves. The surface fluctuations can be expressed by:

$$\zeta(t) = \sum_{n=1}^N \sqrt{2dfS(f_n)} \cdot \cos(\sigma_n t - \varepsilon_n) \quad (15)$$

$$\sigma_n = 2\pi f_n \quad (16)$$

here ε_n and N denotes random variable number between $0 \sim 2\pi$ and total number of sampling, respectively.

The horizontal velocities as well as the boundary conditions on the wave-paddle, i.e. Eq. (8), is therefore obtained by

$$U(t) = \sum_{n=1}^N \sqrt{2dfS_o(f_n)} \cdot \alpha(f) \cdot \cos(\sigma_n t - \varepsilon_n) \quad (17)$$

2.3 Integral Formulation and Boundary Discretization

According to Green's second identity, the velocity potential $\Phi(x,z;t)$ for inviscid and irrotational flow can be obtained by the velocity potential on the boundary, $\Phi(\xi,\eta;t)$, and its normal derivative, $\partial\Phi(\xi,\eta;t)/\partial n$, the continuity equation in differential form, Eq. (1), can thus be transformed into a boundary integral equation as:

$$c\Phi(x,z;t) = \frac{1}{2\pi} \int_{\Gamma} \left\{ \frac{\partial\Phi(\xi,\eta;t)}{\partial n} \ln\left(\frac{1}{r}\right) - \Phi(\xi,\eta;t) \frac{\partial}{\partial n} \left[\ln\left(\frac{1}{r}\right) \right] \right\} ds \quad (18)$$

$$c = \begin{cases} 1 & \text{inside the fluid domain} \\ 1/2 & \text{on the smooth boundary} \\ 0 & \text{outside the fluid domain} \end{cases}$$

$$\text{where } r = \sqrt{(\xi - x)^2 + (\eta - z)^2}.$$

The boundaries, Γ_1 through Γ_5 , are divided into, respectively, N_1 to N_5 discrete linear elements. Discretization schema is exhaustive in Fig.2, coarser meshes were used at both ends of the flume, which were then varied gradually into fine meshes when approaching the middle of the flume. The smallest mesh sizes is adopted as $\Delta x = 0.1h$, where h is the water depth. The computational domains were discretized into, respectively, 10 elements for the pseudo wave-paddle, 5 elements for the vertical wall, 70 elements for the impermeable bottom, 234 elements for the free water surface and 5 elements for each side of the submerged obstacle.

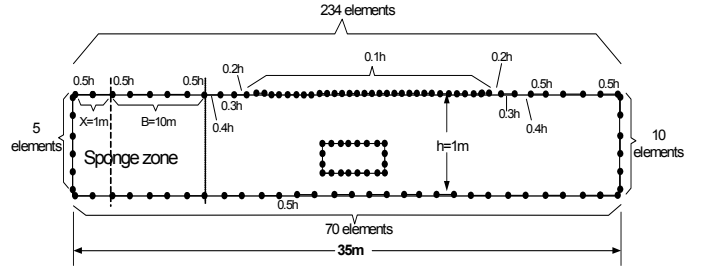


Fig.2 Discretization scheme for computational cases

To proceed with the calculation, Eq.(18) can be expressed in matrix form:

$$[\Phi_i] = [O_{ij}] [\overline{\Phi}_j]; \quad i, j = 1 \sim 5 \quad (19)$$

$[\Phi]$ and $[\overline{\Phi}]$ are, respectively, the velocity potential and its associated normal derivative. The coefficients of the matrix $[O]$ are related to the geometric shapes of the boundaries.

The velocity potential on the boundary of the wave-generator, Φ_1^k , the normal derivative of the velocity potential of the free surface, $\overline{\Phi}_2^k$, and the velocity potentials on the fixed impermeable boundaries, Φ_3^k , Φ_4^k , Φ_5^k at the k -th time step can be obtained by substituting the initial boundary conditions into Equation (19). By differentiating the time derivatives in Eqs.(2), (3), and (4) through forward differencing, the position of nodes are regridded every time step, new positions of the nodes on free water surface, (x^{k+1}, z^{k+1}) can thus be obtained and regridded as:

$$x^{k+1} = x^k + \left(\frac{\partial\Phi_2^k}{\partial x} \right) \Delta t \quad (20)$$

$$z^{k+1} = z^k + \left(\frac{\partial\Phi_2^k}{\partial z} \right) \Delta t \quad (21)$$

and the velocity potential on the free water surface, Φ_2^{k+1} , at the next time step, $t = (k+1)\Delta t$ is given through:

$$\Phi_2^{k+1} = \Phi_2^k + \frac{1}{2} \left[\left(\frac{\partial\Phi_2^k}{\partial s} \right)^2 + \left(\frac{\partial\Phi_2^k}{\partial n} \right)^2 \right] \Delta t - g z^{k+1} \Delta t - \frac{P^k}{\rho} \Delta t \quad (22)$$

where s and n denote, respectively, the tangential and the normal direction. The normal derivatives on the boundaries Γ_1 , Γ_3 , Γ_4 and Γ_5 ,

i.e., $\bar{\Phi}_1^{k+1}$, $\bar{\Phi}_3^{k+1}$, $\bar{\Phi}_4^{k+1}$ and $\bar{\Phi}_5^{k+1}$, at time step $t = (k+1)\Delta t$ can be obtained through the use of Eqs. (8) and (9). These can be written more compactly in a matrix form:

$$\begin{bmatrix} \bar{\Phi}_1 \\ \bar{\Phi}_2 \\ \bar{\Phi}_3 \\ \bar{\Phi}_4 \\ \bar{\Phi}_5 \end{bmatrix}^{k+1} = \begin{bmatrix} I & -O_{12} & 0 & 0 & 0 \\ 0 & -O_{22} & 0 & 0 & 0 \\ 0 & -O_{32} & I & 0 & 0 \\ 0 & -O_{42} & 0 & I & 0 \\ 0 & -O_{52} & 0 & 0 & I \end{bmatrix}^{-1} \begin{bmatrix} O_{11} & 0 & O_{13} & O_{14} & O_{15} \\ O_{21} & -I & O_{23} & O_{24} & O_{25} \\ O_{31} & 0 & O_{33} & O_{34} & O_{35} \\ O_{41} & 0 & O_{43} & O_{44} & O_{45} \\ O_{51} & 0 & O_{53} & O_{54} & O_{55} \end{bmatrix} \begin{bmatrix} \bar{\Phi}_1 \\ \bar{\Phi}_2 \\ \bar{\Phi}_3 \\ \bar{\Phi}_4 \\ \bar{\Phi}_5 \end{bmatrix}^k \quad (23)$$

I is the identity matrix. Detailed description concerning the iterative scheme of time stepping and computational procedures can be found in Chou & Shih (1996).

2.4 Estimation of Reflection Coefficient

The estimation of separating irregular incident and reflected waves in a random wave field are being extensively investigated, e.g. Goda and Suzuki (1976) presented a method for estimation of incident and reflected waves in a random wave field under frequency domain. Mansard and Funke(1980) presented an improved Goda's method by least square techniques, Figaard and Brorsen(1995) further investigated a time-domain method for the separating of irregular waves by use of the digital filters, which are therefore able to separate the wave fields in real time. The reflection coefficients of irregular waves are estimated in this paper presently by utilizing the method of Goda and Suzuki (1976) for separation of incident and reflected wave. Based on the time histories of water elevations measured with numerous pseudo wave gages on the free water surface, the amplitude are analyzed by the FFT technique, thus, the reflection coefficients were estimated as follow:

The composite wave profiles of incident and reflected waves at location $x = x_1$ and $x = x_1 + \Delta l$ can be expressed as:

$$\eta_1 = (\eta_i + \eta_r)_{x=x_1} = A_1 \cos \sigma t + B_1 \sin \sigma t \quad (24)$$

$$\begin{cases} A_1 = a_i \cos \theta_i + a_r \cos \theta_r \\ B_1 = a_i \sin \theta_i + a_r \sin \theta_r \end{cases} \quad (25)$$

$$\eta_2 = (\eta_i + \eta_r)_{x=x_1+\Delta l} = A_2 \cos \sigma t + B_2 \sin \sigma t \quad (26)$$

$$\begin{cases} A_2 = a_i \cos(\theta_i + k\Delta l) + a_r \cos(\theta_r + k\Delta l) \\ B_2 = a_i \sin(\theta_i + k\Delta l) + a_r \sin(\theta_r + k\Delta l) \end{cases} \quad (27)$$

where $\theta_i = kx_1 + \varepsilon_i$, $\theta_r = kx_1 + \varepsilon_r$, k is the wave number, σ is the angular frequency and ε is the phase angle, the subscript "i" and "r" denotes incident and reflected waves, respectively. Δl is the spacing between two measuring stations.

The amplitudes a_i and a_r can thus be calculated by:

$$a_i = \frac{1}{2|\sin k\Delta l|} [(A_2 - A_1 \cos k\Delta l - B_1 \sin k\Delta l)^2 + (B_2 + A_1 \sin k\Delta l - B_1 \cos k\Delta l)^2]^{1/2} \quad (28)$$

$$a_r = \frac{1}{2|\sin k\Delta l|} [(A_2 - A_1 \cos k\Delta l + B_1 \sin k\Delta l)^2 + (B_2 - A_1 \sin k\Delta l - B_1 \cos k\Delta l)^2]^{1/2} \quad (29)$$

The energies of the incident and reflected waves, E_i and E_r could be obtained by:

$$E_i = \int_{f_{\min}}^{f_{\max}} S_i(f) df \quad (30)$$

$$E_r = \int_{f_{\min}}^{f_{\max}} S_r(f) df \quad (31)$$

Consequently, the reflection coefficient, K_r , can be estimated:

$$K_r = \sqrt{\frac{E_r}{E_i}} \quad (32)$$

RESULTS AND DISCUSSIONS

3.1 Absorption of Irregular Waves

As mentioned previously, an artificial absorbing beach represents here as sponge zone is employed at the end of the flume to minimize the reflection effects. The effectiveness of the absorbing boundary are demonstrated by Chou et al. (2002) in the simulations of both solitary and periodic waves, the absorbing coefficient $\mu=1$ was adopted to minimize the reflection effects and is also adopted in the present investigation. According to our investigation, though the efficiency of the sponge zone work successfully on both solitary and periodical waves, the same absorption coefficient might not be well employed for an irregular train of waves, eventhough the absorbing technique is employed in the model, still, a small quantity of reflected wave from the vertical wall, besides, the numerical model became much more complicated after the submerged obstacles was set, the reflected waves cause by the obstacle was unable to be eliminated by the absorbing technics as it was employed at the end of the flume, which inevitably contaminate the incident wave train, including the re-reflection from the wave paddle. This problem can be rudimentary solved by lengthening the flume, poor but efficacious, still, a more effective technique will be discussed prospectively in the further extension. Fig.3~4 revealed respectively the variations of wave profile for non-absorbing ($\mu=0$) and absorbing area ($\mu=1$) cases in a wave flume without obstacle, where $\Delta t = T_{1/3}/200$. As can be seen in the figures, there exist an increasing mean water level in Fig.4, which is not observed in the full reflected ($\mu=0$) case, this is related to the value of absorbing term P/ρ we added, the atmospheric pressure term is generally assumed to be constant, e.g., $P=0$ while $\mu=0$, when an excess artificial pressure is acted on the free surface, due to conservation of energy, velocity potential energies were transferred by the damping term on the free surface, since the value of P was defined proportional to the potential on the free water, it gradually decrease the wave elevation and somehow altered the water level due to the variation of absorbing term.

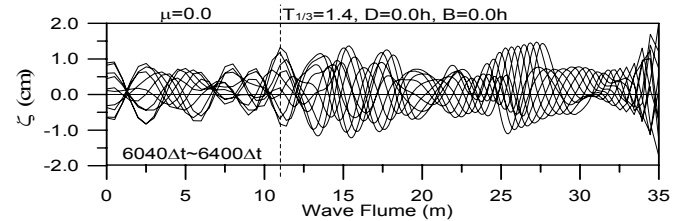


Fig.3 Variations of wave profiles without absorption ($\mu=0$)

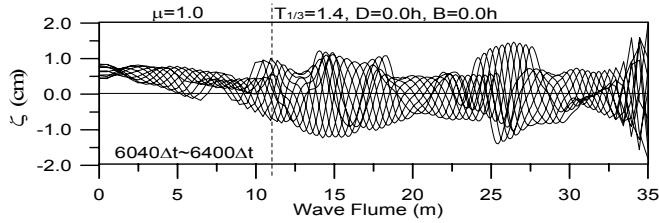


Fig.4 Variations of wave profiles with absorption ($\mu=1.0$)

Under the former circumstances ($\mu=0$), the variation of reflected coefficient is shown in Fig.5 where the significant wave period $T_{1/3}=0.6\sim 1.4$ sec, theoretically, the reflection coefficient should be equal to 1.0 when waves are totally reflected, however, due probably to the nonlinearity and asymmetry, only partial standing wave was form after reflection, consequently, from Fig.5 we acquired satisfactory results except for the case with $T_{1/3}=1.2$ sec where the reflection coefficient is comparatively small.

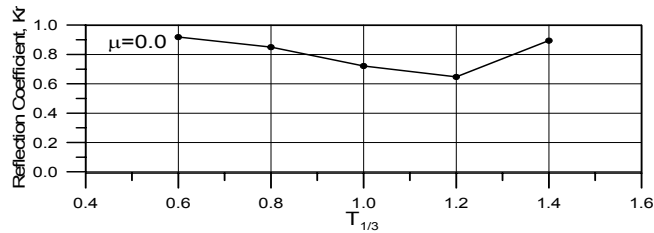


Fig.5 Variations of reflection coefficients without absorption ($\mu=0$)

3.2 Variations of Waveform Relative to Obstacle Length

Fig.6(a)~(d) shows the time series of waveform variations with identical duration, the significant wave period of incident wave and the height of submerged dike are fixed as $T_{1/3}=1.0$ sec and $D=0.5h$, respectively, whereas the length of the dike increases gradually from $B=1h\sim 4h$. As revealed in Fig.6(d), partial standing waves apparently formed in front of the dike when the length B reached $4h$, wave height distributions behind the dike appeared lower range than those of (a)~(c), this may as well superficially denote as the increasing of reflection waves. However, unlike monochromatic waves with stationary frequency, irregular waves are composed of considerable quantities of component waves with different frequencies and heights, the appearance of nodes in wave height envelope was unapparent and mostly never occurred, the estimation of reflection quantity of wave energy by waveform determination as shown in Fig.6 was thus incapable when significant wave period $T_{1/3}$ varies, i.e. the intensity of partial standing waves does not represent reflection quantities. Concerning this problem, Fig.7(a)~(d) represents the case with varying significant wave period $T_{1/3}$ of 0.8sec to 1.4sec, which the length and height of the submerged dike are $B=4h$ and $D=0.5h$ respectively. As revealed, the partial standing waves in front of the dike was conspicuous when $T_{1/3}=0.8\sim 1.0$ sec but rather inconspicuous for the others. To illustrate the above occurrence, the spectra measured at the position before and after the obstacle are shown in Fig.8(a)~(d). According to the case in Fig.9, as the length B increase up to $3h$ when $D=0.75h$, waves will have longer distance to travel over the obstacle and thus will have greater shoaling effect, in fact may lead to wave breaking. The wave damping effect of the submerged dike in case of breaking is remarkably different from that in case of non-breaking; nevertheless, the simulation of breaking of irregular wave is yet incapable and so far not considered in this paper, which discussed merely over non-breaking circumstances.

3.3 Analysis Results of Reflection Coefficient

Reflection coefficient are estimated using the two gauge analysis technique of Goda and Suzuki (1976) by the variations of water elevation, the time histories of surface elevations are measured with a total of 32 pseudo wave gauges, starting from the wave-paddle, Station 1 ~ 32, measuring stations were used to record the developments of the irregular waves along the wave tank. Table 1 lists the number of all stations and their distances from the origin. Though the wave gauges may be located at as near as $0.2L$ (L stands for wavelength) to the obstacles in irregular wave test, it was recommended by Goda and Suzuki to be located at a distance of at least more than one wave length L from both the obstacle and the paddle in irregular wave test. Accordingly, the gauges are combined and distributed into six groups as listed in Table 2, the spacing between every two gauges was employed as $\Delta l=0.5h$.

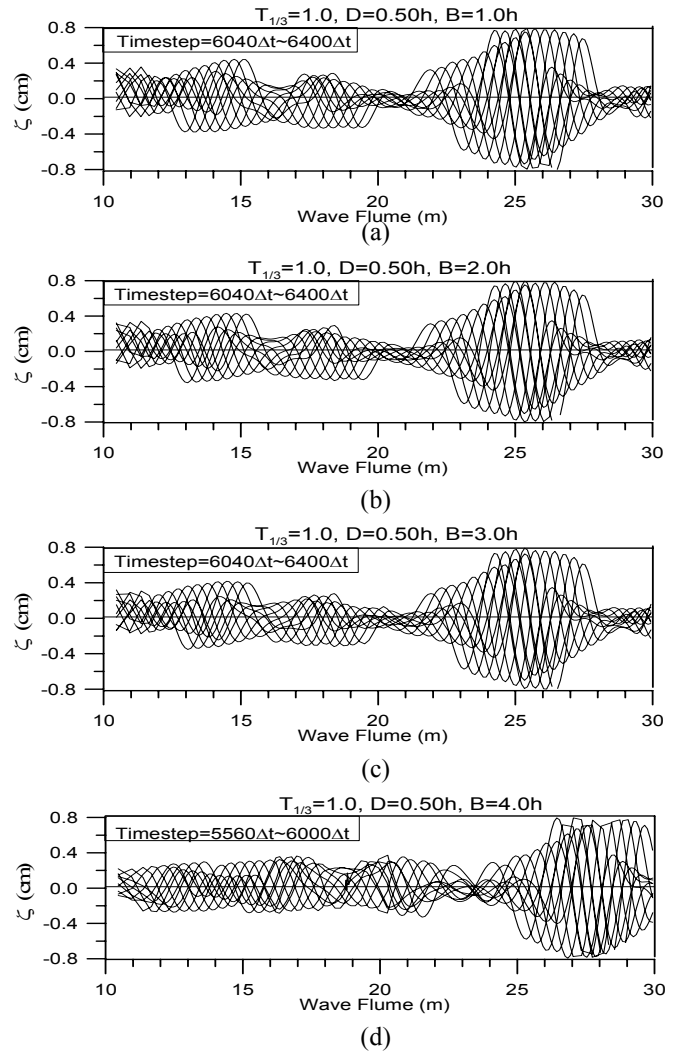


Fig.6 Time histories of water elevations due to submerged obstacles with various lengths, B ($T_{1/3}=1.0$ sec, $D=0.5h$, $\Delta t=T_{1/3}/200$)

As mentioned previously, after the submerged obstacle was located, the waves reflected by the obstacle travel back to the paddle and are re-reflected, these re-reflected waves propagate toward the obstacle and are reflected again, the process may be repeated several times until the

simulation was terminated by accumulating errors. Therefore, to minimize the inaccuracy, the sampling time of data collections for reflection analyzing applied presently is equivalent to the measurement (of reflection coefficient) as adopted practically in the laboratory, i.e. the sampling times started when the reflected waves from the obstacle reached the gauges, and stop before the re-reflected wave from the paddle approached. Due to the reflections and the length of the flume, only short wave data are available for analysis. Though Duclos and Clément (2003) have presents a new method for the calculation of reflection coefficient in a small basin by extending Goda and Suzuki's method to three probes technique, still, the Goda method was utilized in this paper.

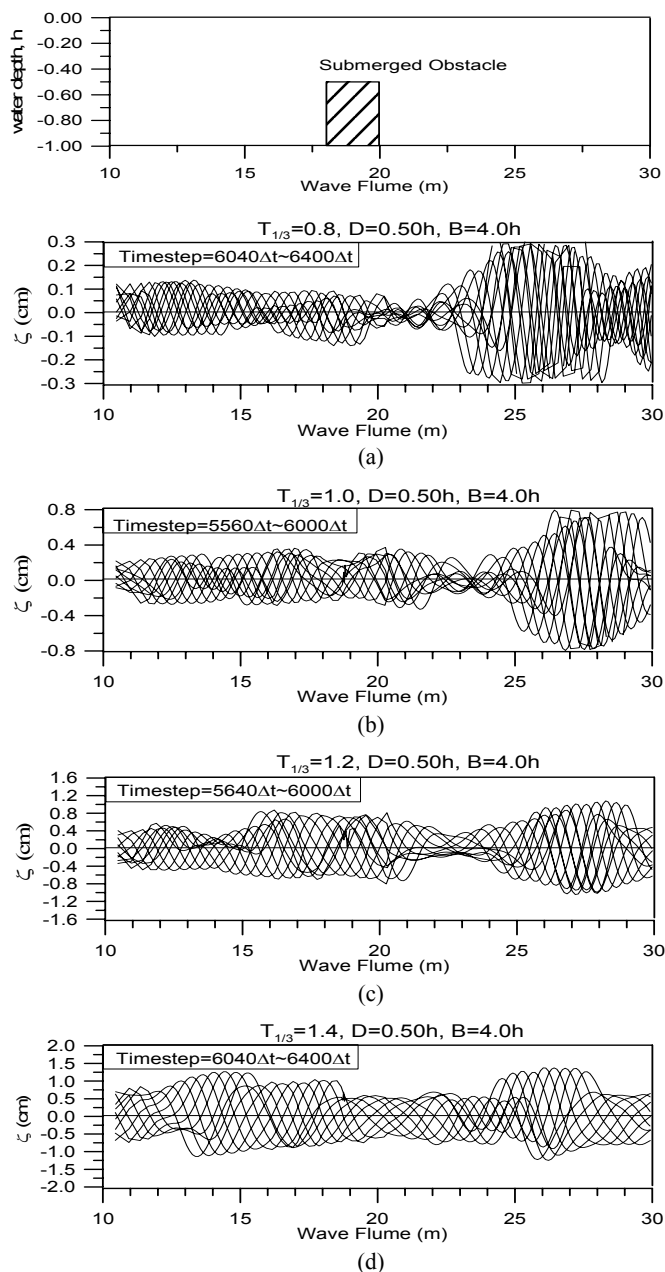


Fig.7 Time histories of water elevations due to submerged obstacles with various significant wave period, $T_{1/3}$ ($D=0.50h$, $B=4h$).

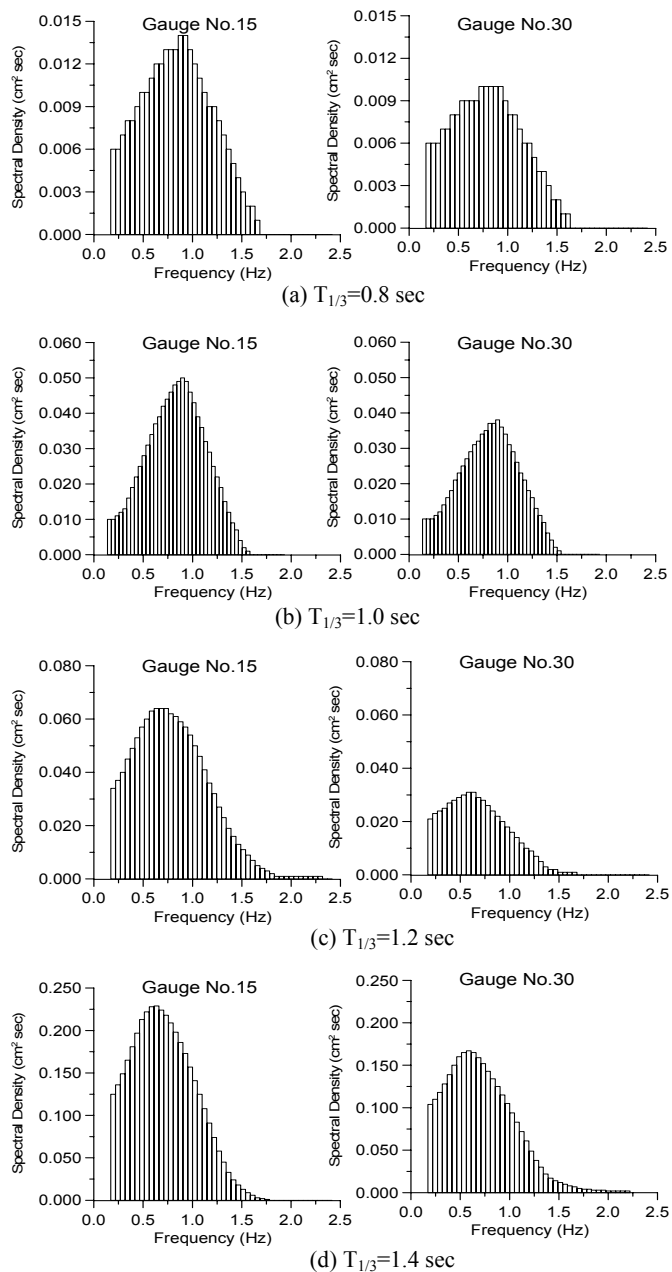


Fig.8 Spectra of irregular waves measured before (gauge No.15) and after (gauge No.30) the obstacle. ($D=0.50h$, $B=4h$)

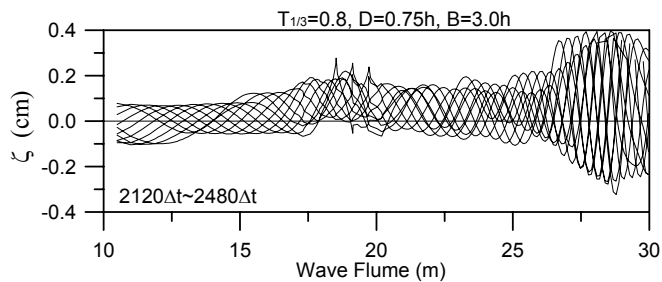


Fig.9 Time histories of water elevations due probably to shoaling by submerged obstacles.

Fig.10(a)-(d) presents the variations of reflection coefficients for irregular wave passing over a submerged dike with identical length B , from which we discovered that when $B \leq 2h$ and $T_{1/3} < 1.0$, the influence of D on Kr seems to be rather small, as (a) and (b) exhibited. Contrarily, as revealed in (c) and (d), except for the case of $T_{1/3} = 0.6$ with $B = 3h$, the reflection coefficient in its entirety apparently increases when $B > 2h$, particularly when the height of dike D reaches $0.75h$. This can also be seen in Fig.11(a)-(c) when the heights of submerged dike D remained identical, the enlargement of the dike's lengths influenced the reflection infirmly under the conditions of $D \leq 0.5h$ and $B \leq 2h$, nevertheless, the reflection coefficients increased relatively with the length of the dike when $D = 0.75h$ and $B = 3h \sim 4h$. By comparing Fig.10 with Fig.11, it is interesting that the reflection coefficients for waves with significant period of $T_{1/3} = 1.2$ possess larger values than the others, which also seems to have the slightest variations. The comparison between the spectra density of incident wave and reflected wave for the cases of $T_{1/3} = 0.8$, $D = 0.50h$, $B = 4h$ and $T_{1/3} = 0.8$, $D = 0.75h$, $B = 1h$ are illustrated by Fig.12, for clarification, the ratio of spectral density (S-d) between incident and reflected wave are shown in Fig.13 as well.

Table 1. Location of wave gauges along the flume

Gauge No.	Location (m)	Gauge No.	Location (m)	Gauge No.	Location (m)	Gauge No.	Location (m)
01	31.0	09	22.7	17	21.9	25	21.1
02	29.0	10	22.6	18	21.8	26	20.0
03	26.0	11	22.5	19	21.7	27	19.0
04	25.0	12	22.4	20	21.6	28	18.0
05	24.0	13	22.3	21	21.5	29	17.0
06	23.0	14	22.2	22	21.4	30	15.0
07	22.9	15	22.1	23	21.3	31	12.0
08	22.8	16	22.0	24	21.2	32	11.0

Table 2. Combination of wave gauges

Group No.	Gauge No. ($\Delta l = 0.5h$)		Group No.	Gauge No. ($\Delta l = 0.5h$)	
01	11	16	04	08	13
02	10	15	05	07	12
03	09	14	06	06	11

CONCLUSION

Applications of numerical wave flume for irregular waves propagate over a set of submerged obstacles with various conditions are investigated in this study by means of BEM. The estimations of reflection coefficients for irregular waves over submerged obstacles exhibited a feasible scheme. Some conclusions may be drawn from the present results as follow:

1. The present numerical scheme is applicable for the estimations of reflection coefficient, estimated results could be regarded as reference material before carrying out hydraulic experiments so as to economize on both the spatial and temporal expenditure.

2. Numerical modelling has become much more complicated after the submerged obstacles was located, the reflected waves cause by the obstacle was unable to be eliminated by the absorbing technics employed at the end of the flume, which then travel back to the paddle and are re-reflected, these re-reflected waves are presently reflected again by the obstacle, the repeated process may cause great errors to the estimations, furthermore, the flume adopted presently was 35m in

length, the longest wave may be up to 13m according to the selected period (0.5~0.45sec), which indicated that the length of the flume is less than 3 complete wavelength, this may greatly affects the accuracy of the results, therefore, excluding lengthened the flume, a development of the present wave paddle into a so-called "absorbing wave maker" is imperative and will be consider prospectively.

3. Inappropriate positions of wave gauges with different combinations may occur greater discrepancies in the estimations, which in this case should be avoid. The reflection coefficient for each case are obtained by averaging the estimated results of each cases, though little discrepancies may occur between each combination, the variation tendency in its entirety is in unanimity.

4. The reflection coefficients increased relatively with the length of the dike when $D > 0.5h$ and $B > 2h$, nevertheless, the lengthening of dike's lengths influenced the reflection infirmly when $D \leq 0.5h$ and $B \leq 2h$.

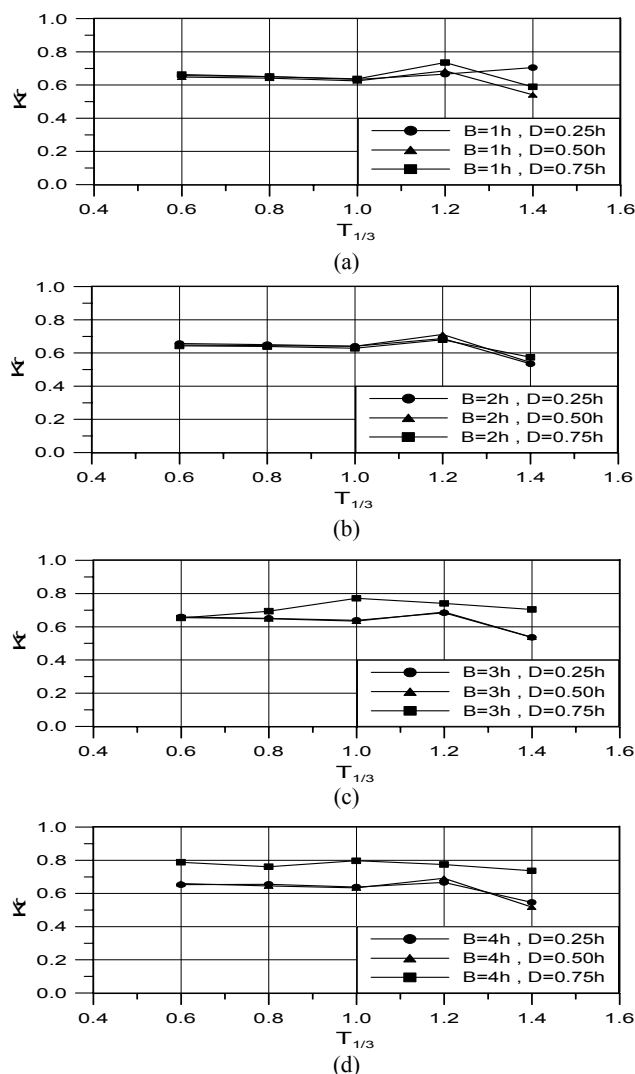


Fig.10 Comparison of reflection coefficients variations between various obstacles heights, D

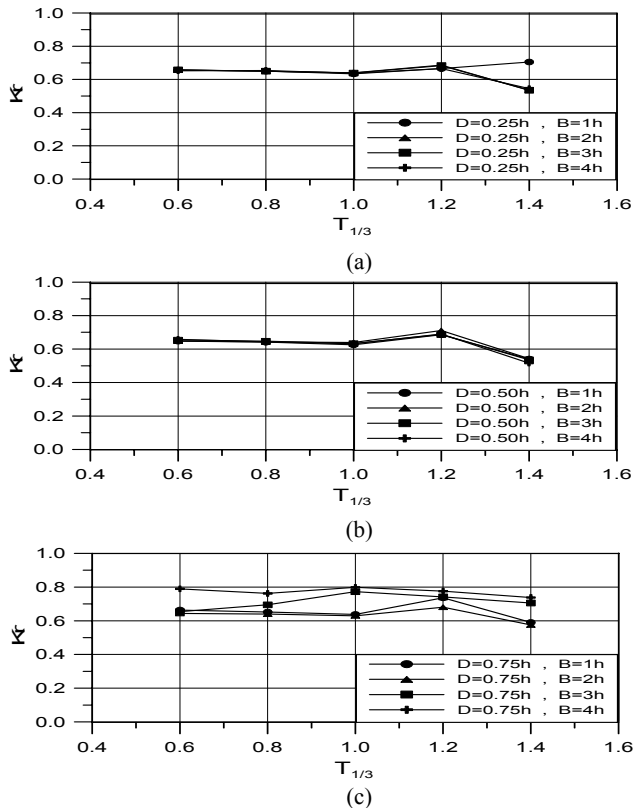


Fig.11 Comparison of reflection coefficients variations between various obstacle lengths, B

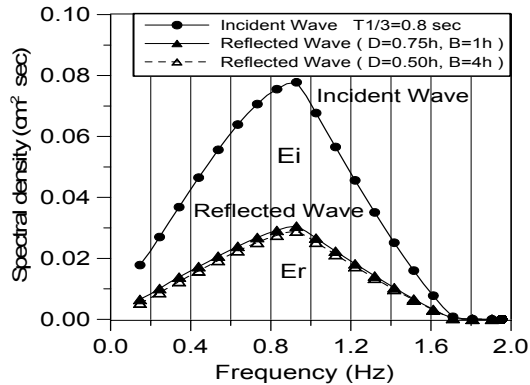


Fig.12 Spectral density of the incident and reflected wave.

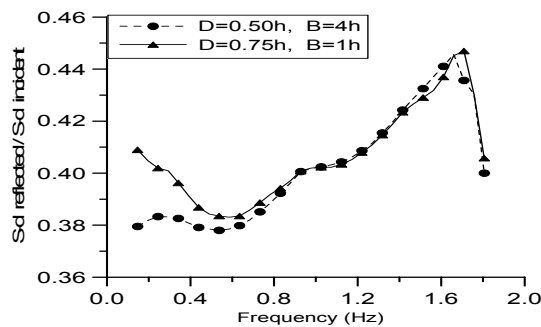


Fig.13 Ratio of spectral density (S-d) between incident and reflected wave. ($T_{1/3}=0.8$)

ACKNOWLEDGEMENTS

The authors wish to express their gratitude for the financial aids of the National Science Council, Republic of China, Project No. NSC-92-2611-E-236-001.

REFERENCES

- Baldock, T.E. and Simmonds, D.J. (1999) "Separation of incident and reflected waves over sloping bathymetry", *Coastal Engineering*, Vol.38, pp.167~176.
- Cao, Y., Beck,R.F. & Schultz, W.W. (1993) "An absorbing beach for numerical simulations of nonlinear waves in a wave tank", *Proc. 8th Intl. Workshop Wavter and Floating Bodies*. pp.17~20.
- Chou, C.R. and Ouyang, K. (1998) "Development of numerical irregular wave making channel", *Pro. Of the 8th China-Japan symposium on Boundary Element Method*, Acadmic Publisher, pp.142~149.
- Chou, C.R. and Shih, R.S. (1996) "Generation and deformation of solitary waves", *China Ocean Eng.*, China Ocean Press, Vol.10, No.4, pp.419-432.
- Chou, C.R. Shih, R.S and Yim, Z. John. (2001) "'A numerical wave tank for nonlinear waves with passive absorption", *China Ocean Engineering*. Vol.15, No.2, pp.253~268.
- Chou, C.R. Shih, R.S and Yim, Z. John. (2002) "Optimizing deployment of sponge zone on numerical wave channel", *Journal of the Chinese Institute of Engineers*. Vol. 25, No.2, pp.147-156.
- Duclos, G., and Clément A.H. (2003) "A new method for the calculation of transmission and reflection coefficients for water waves in a small basin", *Comptes Rendus Mecanique*", Elsevier Press, Vol.331, pp.225~230.
- Figaard, P. & Borsen, M. (1995) " A time-domain method for separating incident and reflected irregular waves", *Coastal Eng.*, Vol.24, pp.205~215.
- Gaillard, P., Gauthier, M. and Holly, F. (1980) "Method of analysis of random wave experiments with reflecting coastal structures", *Proc. 17th Int. Conference on Coastal Engineering*, Sydney, Vol.1, pp.204~220.
- Goda Y. (2000) 'Random Seas and Design of Maritime Structures', Advance Series on Ocean Engineering. World Scientific.
- Goda, Y. and Suzuki, Y. (1976) " Estimation of incident and reflected waves in random wave experiments", *Proc. 15th Int. Conference on Coastal Engineering*, Honolulu, Vol.1, pp.828~845.
- Lee, T.T. and Black, K.P. (1978) "The energy spectra of surf waves on a corel reef", *Proc. 16th Int. Conference on Coastal Engineering*, Vol.1, pp.588~608.
- Mansard, E. and Funke, E. (1980) "The measurement of incident and reflected spectra using a least square method", *Proc. 17th Int. Conference on Coastal Engineering*, Sydney, Vol.1, pp.154~172.
- Nakamura, N., Shiraiishi, H. and Sasaki, Y. (1966) "Wave damping effect of submerged dike", *Proc. 10th Int. Conference on Coastal Engineering*, Vol.1, pp.254~267.
- Sanchez, M. (2000) "Estimation du coefficient de réflexion en canal à houle", *C.R. Acad. Sci. Paris, t. 328, Série II b*, pp.883~889.
- Shih, R.S., Chou, C.R. and Yim, Z. John. (2004) "Numerical Investigation on the Generation and Propagation of Irregular Waves in a Two Dimensional Wave Tank", *China Ocean Engineering*, Vol.18, No.4, pp.551-566.
- Shu, K.D., Choi, J.C., Kim, B.H., Park, W.S. and Lee, K.S (2001) "Reflection of irregular waves from perforated-wall caisson breakwaters", *Coastal Engineering*, Vol.44, pp.141~151.